Analytical Study for a Set of Partially Strengthened End-Bearing Granular Piles

A. Jitendra Kumar Sharma[1] and B. Ashish Solanki[2]
[1]*Professor and HOD, Department of Civil Engineering, Rajasthan Technical University, Kota, India*
[2] *Ph.D. Research Scholar, S.M., ASCE, IGS, Department of Civil Engineering, Rajasthan Technical University, Kota, India*
E-mail: jksharma@rtu.ac.in[1]

ABSTRACT: In the modern era, the demand of construction is getting high, but land resources are getting exhausted and sometimes left behind option is to use soft soil, which requires ground improvement. Granular Piles (GP) are the most efficient and reasonable key for this problem. In this paper, a comparative study of a set of partly strengthened end-bearing GPs is presented, unfolding the comparison between analytical and rigorous analysis for several normalized aspects like displacement effecting component (D_E) for top of GP, displacement interaction factor, percentage load shared by the base (PLSB) and values of normalized shear stress (NSS) across the length of the GP are assessed for end bearing set of two, three, four uniformly placed end bearing piles. The D_E, for top of GP is noticed to get decline with the intensification in the values of the strengthening parameters. The interfacial shear stresses get reorganized along the length of the GP.

KEYWORDS: End bearing GP, Displacement effecting component (D_E) for top of GP, Displacement interaction factor, Strengthening length fraction from top of GP, Strengthening factor for top of GP.

1. INTRODUCTION

In the present situation of the current reality where land accessibility is diminishing step by step, construction on soft soil is an enforced choice and for increasing its load-bearing capacity, the ground improvement technique is used by means of GP. As compared to conventional GP here in this analysis, partial strengthening is done at the top portion of the GP so as to get rid of the problem of bulging occurring in the top portion of conventional GP. The partial strengthening may be done by geosynthetic encasement, SDCM (stiffened deep cement mixing), etc. In the present study, the comparative analysis of a set of two, three, and four partly strengthened end-bearing GPs, individually loaded with an axial load, 'F', partly strengthened, is worked out using the elastic continuum approach. It is established by the present study that increasing the strengthening factor leads to increase in the load-bearing capacity of different set of GPs.

The analysis is based on the following assumptions

1. Stress vs. strain relationship is supposed to be rectilinear.
2. Surrounding soft soil is supposed to have homogeneity and isotropic property. Its behavior is also assumed as rectilinear elastic.
3. In order to have uniform distribution of load across the base, the base of GP is assumed to be smooth. (Madhav et al., 2006).
4. The existing work has been carried out by presuming no slip or yield state.

2. LITERATURE SURVEY

From the ancient time of civilization, a number of researchers have worked in the area of ground improvement techniques. But among all those mathematical and experimental investigation techniques adopted, one cannot forget the contribution of the pioneer idea of Mattes and Poulos (1969). Based on the assumption that the reinforcing inclusions are regularly distributed throughout the soil mass and parameters like area ratio, soft soil characteristics, etc., various design charts were developed by Madhav and Nagpure (1995). For upgrading the in situ ground conditions, the involvement of columnar constructions not only replaced the other conventional approaches but also leads to an economic and versatile strategy for ground improvement techniques Alamgir et al. (1996). A study was conducted by Poorooshasb et al. (1998) on two types of column, i.e., plain and reinforced (encased) and an upper bound analysis was proposed for the settlement of the systems of foundations having stone columns included with them, considering the non-linear behavior of the surrounding soft clay. By conducting laboratory experiments, Sivakumar et al. (2004) studied the load-deformation performance of specimens of soft clay reinforced with single sand columns with various lengths. A well-organized analytical model was developed by Pulko and Majes (2005) to forecast the settlements in a widespread rigid foundation supported by end-bearing stone columns. The study, based on FEM (finite element method), conducted by Murugesan and Rajagopal (2006), was a milestone to study the effect of encasing stone columns with geosynthetic material, not only for enhancement in the load-carrying capacity of the stone columns but simultaneously getting rid of the problem of bulging of the granular piles. Small-scale model tests of floating stone columns group were carried out by Shahu and Reddy (2011). This study explored out the parameters like area ratio, over-consolidation ratio, length of column, etc., which affects the behaviour of groups of granular piles. Settlement computations were carried out by Zhang et al. (2012) for composites foundation reinforced with stone columns. For a precise particular condition of reinforcement, it was exposed by Najjar and Skiene (2015) that as related to drained conditions, un-drained conditions prime to upgradation of load-carrying capacity. Garg and Sharma (2019) analytically carried out the settlement analysis of a single and group of two partially floating granular piles. Madhav et al. (2019) presented the analytical solution for studying the settlement analysis of a group of two partially stiffened end-bearing GPs and revealed the advantageous effect of partial stiffening in increasing the load-sharing characteristic of the base of the GP.

3. DESCRIPTION OF THE PROBLEM

The current hitch is revealed in Figure 1 (a) and (b) here, a set of two, end bearing, partly strengthened and individual piles of length 'L_p' and diameter 'D_p'= (2a), such that individual GP is carrying a load 'F' which is axial, is shown. The center-to-center spacing of two GPs is assumed to be 'S_p'. In Figure 2 (a) and (b) a set of three, end bearing and partly strengthened GPs individual pile of length 'L_p' and diameter 'D_p'= (2a), carrying an axial load 'F' is shown. In Figure 3, interfacial shear stresses on soil on a set of three uniformly positioned partly strengthened end-bearing GPs are shown. Likewise, in Figure 4 (a)and (b), a set of four, end bearing and partly strengthened GPs, each of length 'L_p' and diameter 'D_p'= (2a), each GP is carrying an axial load, 'F,' evenly placed, are shown. The top section of respective GP is strengthened up to about certain length 'L_t', $\eta_t = (L_t/L_p)$, strengthening the length fraction from top of GP. The Young's

modulus of the GP in the un-strengthened section is taken as 'E_{pust}'. The immediate soft soil is characterized by Young's modulus, 'E_s' and the Poisson's ratio of soil, 'ν_{ss}'. The RS_p of GP is described as = E_{pust}/E_s, i.e., the ratio of Young's modulus of GP to that of the soil. Correspondingly the relative stiffness of the bearing stratum RSBS is defined as E_{sb}/E_s, where E_{sb} is the modulus of deformation of the bearing stratum. A factor, 'χ_t' (Strengthening factor for top of GP) of which values is taken as more than one is clear to take into account the strengthening, i.e., 'χ_t' is the factor by which the RS_p of the un-strengthened part of individual GP in the GP set is multiplied to get the RS_p of the strengthened part of the GP.

4. SOIL DISPLACEMENT

The integration scheme for equation (Mindlin 1936, 1937) is used. Displacement nodes are taken at the inward side of GP in command to have the extreme effect of the interaction of interfacial shear stresses base pressures for set. Baser of the GP is supposed to be smooth, across which the load is uniformly distributed. Thus, soil displacement equations for a granular pile which is end-bearing, is given by Mattes and Poulos (1969).

For a single-end bearing pile

$$\{\rho^s\} = \left\{\frac{S^s}{D_p}\right\} = \left[[IF^{sp}] - \kappa\left[IF^{spim}\right]\right] \times \left\{\frac{\tau}{E_s}\right\} \quad (1)$$

For two granular pile sets resting on a stiff bearing stratum, the soil displacement equations are

$$\{\rho^s\} = \left\{\frac{S^s}{D_p}\right\} = \left[[_1IF^{sp}] + [_2IF^{sp}] - \kappa[_1IF^{spim}] - \kappa[_2IF^{spim}]\right] \times \left\{\frac{\tau}{E_s}\right\} \quad (2)$$

Similarly, for a set of three granular piles resting on a stiff bearing stratum, the soil displacement equations are

$$\{\rho^s\} = \left\{\frac{S^s}{D_p}\right\} = \left[[_1IF^{sp}] + 2 \times [_2IF^{sp}] - \kappa[_1IF^{spim}] - 2 \times \kappa[_2IF^{spim}]\right] \times \left\{\frac{\tau}{E_s}\right\} \quad (3)$$

For set of four granular piles resting on stiff bearing stratum, the soil displacement equations are

$$\{\rho^s\} = \left\{\frac{S^s}{D_p}\right\} = \begin{bmatrix}[_1IF^{sp}] + [_2IF^{sp}] + [_3IF^{sp}] + [_4IF^{sp}] \\ -\kappa[_1IF^{spim}] - \kappa[_2IF^{spim}] - \kappa[_3IF^{spim}] - \kappa[_4IF^{spim}]\end{bmatrix} \times \left\{\frac{\tau}{E_s}\right\} \quad (4)$$

Due to uniformity of places of GPs, 2, and 3, $[_3IF^{sp}] = [_2IF^{sp}]$ and thus soil displacement equations are

$$\{\rho^s\} = \left\{\frac{S^s}{D_p}\right\} = \begin{bmatrix}[_1IF^{sp}] + 2 \times [_2IF^{sp}] + [_4IF^{sp}] + \\ -\kappa[_1IF^{spim}] - 2 \times \kappa[_2IF^{spim}] - \kappa[_4IF^{spim}]\end{bmatrix} \times \left\{\frac{\tau}{E_s}\right\} \quad (5)$$

Where $\{S^s\}$ and $\{\rho^s\}$ are soil displacement and normalized soil displacement $\{\rho^s\}$ is of size 'n' for end bearing GPs, $\{\tau/E_s\}$ is a column vector of size (n+1), respectively. To account for the effect of the bearing stratum, the mirror image approximation (Mattes and Poulos, 1969) is taken into account, which is shown in Figure 5. The effect of the mirror image elements is taken as κ, times the effect of shear stresses on the real elements in the negative direction, where κ is a non-dimensional parameter that accounts for the compressibility of the base and its value is taken as 1 for GP resting on a rigid stratum correspondingly. $[IF^{sp}]$, $[IF^{spim}]$ is a square matrix of soil D_E of size 'n' for end-bearing GP and soil displacement influencing coefficient due to image elements of size 'n', respectively. Similarly, for a set of two GPs $[[_1IF^{sp}] + [_2IF^{sp}] - \kappa[_1IF^{spim}] - \kappa[_2IF^{spim}]]$, is a matrix of soil displacement influencing coefficient of size 'nxn' for end-bearing granular piles. $[_1IF^{sp}]$ and $[_2IF^{sp}]$ are matrices of influence due to shear stresses on own and adjacent GPs, respectively, while $[_1IF^{spim}]$ and $[_2IF^{spim}]$ are soil displacement influencing coefficient due to, respectively, shear stresses on imaginary elements on own and adjacent GP. Likewise, for a set of three GPs $[[_1IF^{sp}] + 2x[_2IF^{sp}] - \kappa[_1IF^{spim}] - 2x\kappa[_2IF^{spim}]]$, is a square matrix of soil displacement influencing coefficient of size 'n' for end-bearing granular piles. $[_1IF^{sp}]$ and $[_2IF^{sp}]$ are matrices of influence due to shear stresses on own and adjacent GPs correspondingly, while $[_1IF^{spim}]$ and $[_2IF^{spim}]$ are soil displacement influencing coefficient due to, respectively, shear stresses on imaginary elements on own and adjacent GP. Equally for the case of set of four GPs $[_1IF^{sp}]$, $[_2IF^{sp}]$, $[_3IF^{sp}]$, and $[_4IF^{sp}]$ are square matrices of size (n+1) individually due to the effect of elemental shear stresses of own (first), second (for spacing S_p), third (for spacing S_p) and fourth GP (for spacing $\sqrt{2}S_p$). All the other terms of the equation are already defined in the analysis.

GP displacements for end bearing GP resting on relatively stiff bearing stratum are obtained as follows:

Displacement of the base of a GP resting on a bearing stratum of finite compressibility is approached by Boussinesq's equation for the displacement of a rigid circular disc on a semi-infinite mass as

$$\rho_b^p = \frac{S_b^p}{D_p} = \frac{\frac{p_b(1-\nu_b^2)\pi}{4}}{E_{sb}} \quad (6)$$

By the symmetry equation, the base pressure is stated in terms of shear stresses as

$$p_b = \frac{F}{\frac{\pi D_p^2}{4}} - \frac{4\left(\frac{L_p}{D_p}\right)}{n}\sum_{j=1}^{j=n}\tau_j \quad (7)$$

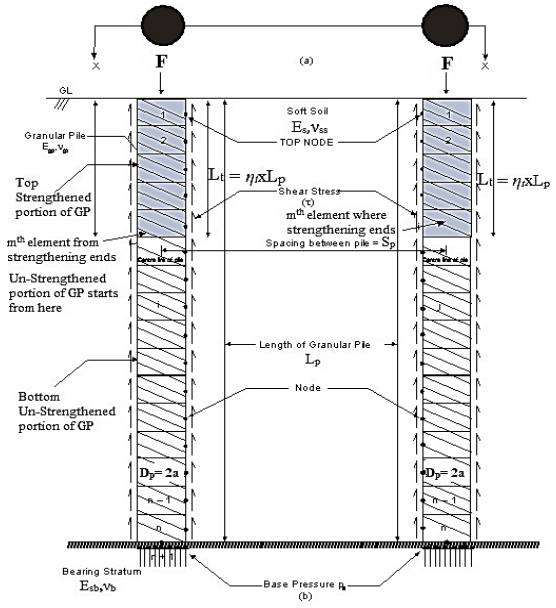

Figure 1(a) Plan of a set of two partly strengthened end-bearing GPs, (b) Front view sectioned at X-X of a set of two partly strengthened end-bearing GPs.

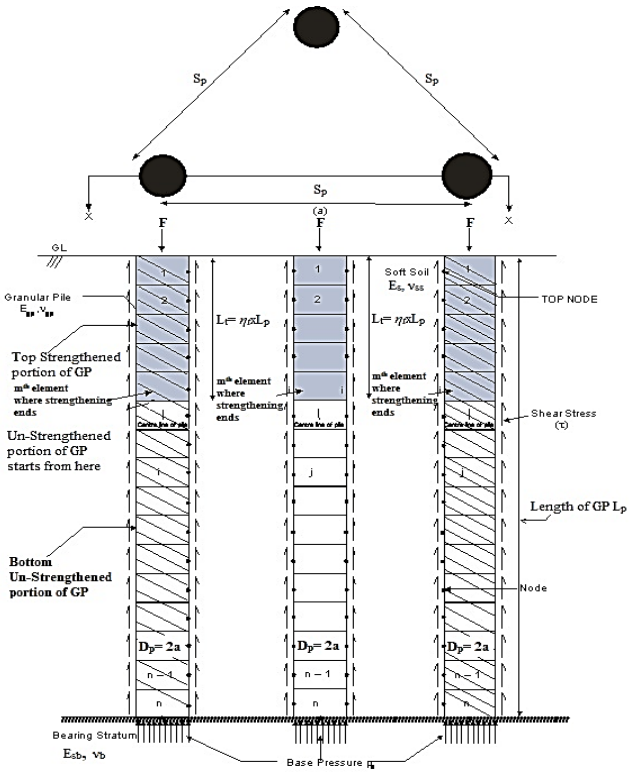

Figure 2 (a) Plan of a set of three uniformly positioned partly strengthened end-bearing GPs, (b) Front view sectioned at X-X of a set of three uniformly placed partly strengthened end-bearing GPs

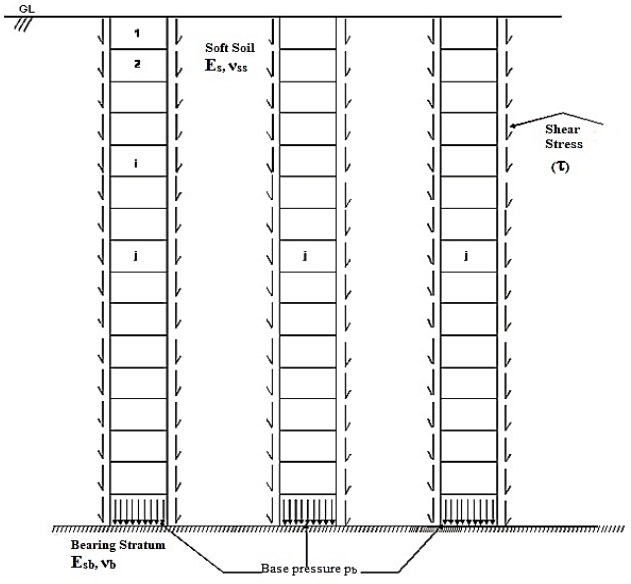

Figure 3 Problematic description plan, interfacial shear stresses on soil on a set of three uniformly positioned partly strengthened end bearing GPs

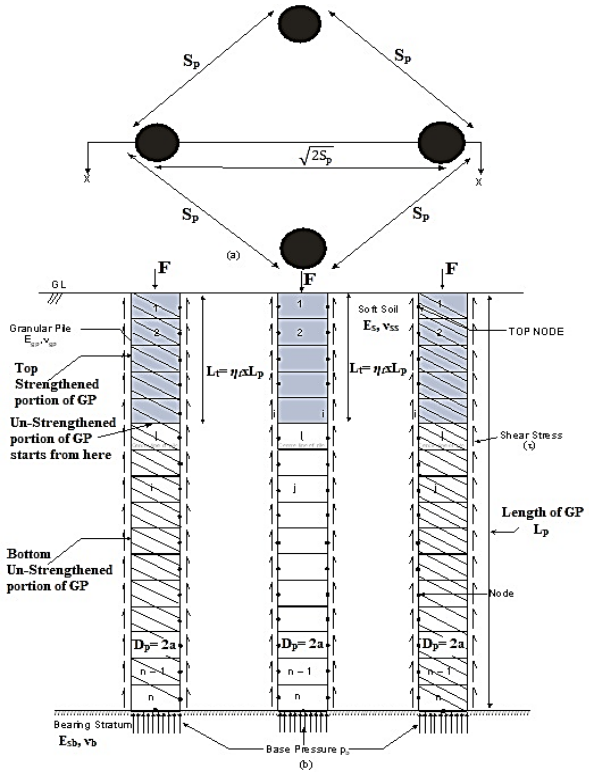

Figure 4 (a) Plan of a set of four uniformly positioned partly strengthened end bearing GPs, (b) Front view sectioned at X-X of a set of four uniformly positioned partly strengthened end bearing GPs

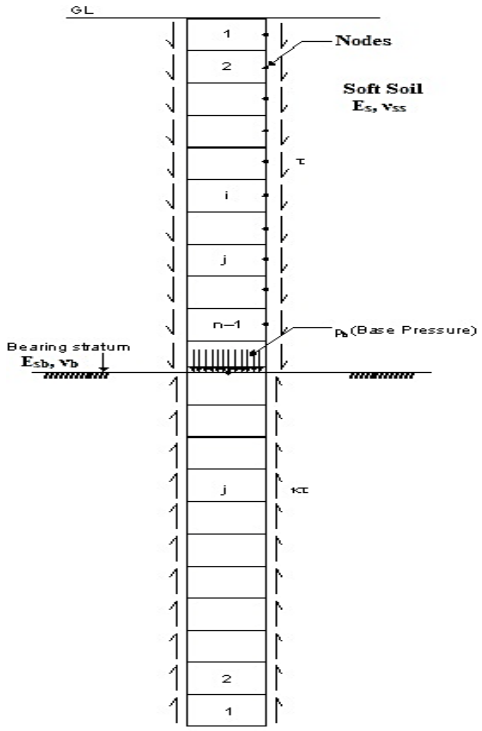

Figure 5 Mirror image procedure for a GP

So the displacement of the base can be stated in relation of the applied load and mobilized shear stresses (using Eq.s (6 and 7) as

$$\rho_b = \left[\frac{F}{\frac{E_s \pi D_p^2}{4}} - \frac{4\left(\frac{L_p}{D_p}\right)}{n}\sum_{j=1}^{j=n}\frac{\tau_j}{E_s}\right] \times \frac{\pi\left(1-\nu_b^2\right)}{4\left(\frac{E_{sb}}{E_s}\right)} \quad (8)$$

Displacement of n^{th} element is assessed as the displacement of the base addition to the displacement of the element due to the axial stress acting on it as:

$$\rho_n^p = \rho_b^p + \frac{\sigma_n\left(\frac{\Delta z_p}{2D_p}\right)}{E_p} \quad (9)$$

Where σ_n/E_p is axial strain of the n^{th} element and Δz_p is the element length. Thus, the displacement of any element i of GP is:

$$\rho_i^p = \rho_b^p + \sum_{j=n}^{j=i-1}\frac{\sigma_j}{E_{pj}\left(\frac{\Delta z_p}{D_p}\right)} + \frac{\sigma_i}{E_{pi}\left(\frac{\Delta z_p}{2D_p}\right)} \quad (10)$$

Due care is observed to keep the compatibility of displacements at the interface or continuity of displacement at the interface of strengthened and un-strengthened portions of GP.A supposition is made that the strengthening is done until the termination of the m^{th} element from the top of the GP as shown in Figures1(b)-2(b)-4(b). The displacement at the bottom of the m^{th} element or top of $(m+1)^{th}$ element, i.e., the interface of a strengthened and un-strengthened portion of GP as given below:

$$\rho_{\text{interface}}^p = \rho_b^p + \sum_{j=n}^{j=m+1}\frac{\sigma_j}{E_{pust}\left(\frac{\Delta z_p}{D_p}\right)} \quad (11)$$

where, $E_{pust,}$ is the Young's modulus of un-strengthened portion. Now the displacement of the bottom end of the m^{th} element of strengthened section is taken as the displacement of the top of the $(m+1)^{th}$ element of un-strengthened section of GP in order to gratify the compatibility at interface amid two. The displacement of center node of m^{th} element is assessed as:

$$\rho_{i=m}^p = \rho_b^p + \sum_{j=n}^{j=m+1}\frac{\sigma_j}{E_{pust}\left(\frac{\Delta z_p}{D_p}\right)} + \frac{\sigma_i}{E_{pst}\left(\frac{\Delta z_p}{2D_p}\right)} \quad (12)$$

where, $E_{pst,}$ is the Young's modulus of strengthened section of the GP. The above set of displacement equations are stated in matrix form as:

$$\{\rho^p\} = \rho_b\{1\} + [\Delta_1]\left\{\frac{\sigma}{E_s}\right\} \quad (13)$$

where $[\Delta_1]$ described later by (Eq. (19) is upper triangular matrix as per Eq. (10), including the strengthening parameters of the GP. Further, by means of Eq.(8) for substituting the base displacement, Eq. (13) can be stated as:

$$\{\rho^p\} = \frac{F\left(1-\nu_b^2\right)}{\left(\frac{E_{sb}}{E_s}\right)D_p^2 E_s}\{1\} - \frac{\pi\left(\frac{L_p}{D_p}\right)\left(1-\nu_b^2\right)}{n\left(\frac{E_{sb}}{E_s}\right)}[1]\left\{\frac{\tau}{E_s}\right\} + [\Delta_1]\left\{\frac{\sigma}{E_s}\right\} \quad (14)$$

whereas {1} and [1] are correspondingly column vectors and square matrices of size 'n' in which the individual term is 1. The shaft shear stresses and axial stresses of elements are linked (based on an equilibrium relationship) as:

$$\sigma_i = \frac{F}{\left(\frac{\pi D_p^2}{4}\right)} - \sum_{j=1}^{j=i-1}\frac{4\tau_j L_p}{nD_p} - \frac{2\tau_i L_p}{nD_p} \quad (15)$$

The above equation may be stated in a matrix system for elements i = 1 to n as:

$$\left\{\frac{\sigma}{E_s}\right\} = \frac{F}{\left(\frac{\pi D_p^2}{4}\right)E_s} - \frac{4\left(\frac{L_p}{D_p}\right)}{n}[\Delta_2]\left\{\frac{\tau}{E_s}\right\} \quad (16)$$

where $[\Delta_2]$ is lower triangular matrix of size 'n' in which the crosswise and off-crosswise terms are 0.5 and 1.0 correspondingly. By means of the relationship amid axial stresses and shaft shear stresses (Eq. 16), the final form of displacement equations for elements i = 1 to n in terms of shaft shear stresses (Eq. 16) are:

$$\{\rho^p\} = \{Y\} + [\Delta]\left\{\frac{\tau}{E_s}\right\} \quad (17)$$

where

$$\{Y\} = \frac{F\left(1-\nu_b^2\right)}{\left(\frac{E_{sb}}{E_s}\right)D_p^2 E_s}\{1\} + \frac{F}{\left(\frac{\pi D_p^2}{4}\right)E_s}[\Delta_1]\{1\}$$
$$[\Delta] = -\frac{4\left(\frac{L_p}{D_p}\right)}{n}[\Delta_1][\Delta_2] - \frac{\pi\left(\frac{L_p}{D_p}\right)\left(1-\nu_b^2\right)}{n\left(\frac{E_{sb}}{E_s}\right)}[1] \quad (18)$$

Over $[\Delta_1]$ is clear below, i.e., a matrix of size (nxn)

$$[\Delta_1] = \frac{\left(\frac{L_p}{D_p}\right)}{nRS_p}\begin{bmatrix} \frac{0.5}{\chi_t} & \frac{1}{\chi_t} & \frac{1}{\chi_t} & 1 & - & - & - & - & 1 \\ 0 & \frac{0.5}{\chi_t} & \frac{1}{\chi_t} & 1 & - & - & - & - & 1 \\ 0 & 0 & \frac{0.5}{\chi_t} & 1 & - & - & - & - & 1 \\ 0 & 0 & 0 & 0.5 & - & - & - & - & 1 \\ . & . & . & . & . & . & . & . & . \\ 0 & 0 & 0 & 0 & 0.5 & 1 & 1 & 1 & 1 \\ 0 & 0 & 0 & 0 & 0 & 0.5 & 1 & 1 & 1 \\ . & . & . & . & . & . & . & . & . \\ 0 & 0 & 0 & 0 & 0 & 0 & 0 & 0 & 0.5 \end{bmatrix}\begin{bmatrix} \text{Here } RS_p \text{ will be replaced by } \chi_t RS_p \text{ for top elements of GP to take into consideration the effect of strengthening upto a depth } \frac{\eta L_p}{D_p} \text{ from top of GP} \end{bmatrix} \quad (19)$$

5. COMPATIBILITY OF DISPLACEMENTS OF SOILAND GP

Filling the compatibility of vertical displacements of the GP and the soil, results are found in terms of interface shear stresses and base pressure. For GP resting on stiff bearing stratum (Eq.s (1) and (17)), the interface shear stresses are:

$$\left\{\frac{\tau}{E_s}\right\} = \left[[IF^{sp}] - \kappa\left[IF^{spim}\right] - [\Delta]\right]^{-1}\{Y\} \quad (20)$$

For an approximation of, κ, an iterative system proposed by Mattes and Poulos (1969) is used. With early chosen values of, κ, Eq.s (20) and (7) are unraveled to approximation the 'n' unidentified shear stresses, τ and base pressure, p_b. Having gotten the result for chosen values of, κ, a nearer approximation of the precise values of, κ, is gotten by taking the compatibility between displacements of soil and the bearing stratum at the pile tip. The soil displacement at the pile tip is:

$$\rho_b^s = \frac{S_b^s}{D_p} = \left\{IF_j^{sb} - \kappa IF_j^{sbim}\right\}\left\{\frac{\tau}{E_s}\right\} = \frac{\sum_{j=1}^{j=n}\left(IF_j^{sb} - \kappa IF_j^{sbim}\right)\tau_j}{E_s} \quad (21)$$

IF_j^{sb} and IF_j^{sbim} are the displacement influencing coefficients for the tip due to shear stresses on real and imaginary elements j respectively. Though due to uniformity $IF_j^{sb} = IF_j^{sbim}$. Equating the soil displacement at the pile tip to the displacement of the base due to base stress, p_b (Eq.6), the new values of the parameter, κ, is found as:

$$\kappa = 1 - \frac{\pi\left(1-\nu_b^2\right)p_b}{4\left(\frac{E_{sb}}{E_s}\right)\sum_{j=1}^{j=n}\tau_j IF_j^{sb}} \quad (22)$$

Now Eq. (20) is resolved iteratively by means of the new values of, κ and the procedure is repeated till the essential convergence is attained for the values of, κ. Here essential convergence means that the percentage difference amid the new values of, κ and last calculated values of, κ, is 0.01%.

The ongoing discussion was in context to a single partly strengthened GP. In the upcoming section same analysis is repeated for a set of two/three/four partly strengthened GPs with slight modifications as described below. For a two-granular pile set resting on stiff bearing stratum (Eq.s (17) and (2), the interface shear stresses are:

$$\left\{\frac{\tau}{E_s}\right\} = \left[\left[{}_1IF^{sp}\right] + \left[{}_2IF^{sp}\right] - \kappa\left[{}_1IF^{spim}\right] - \kappa\left[{}_2IF^{spim}\right]\right] - [\Delta]\Big]^{-1}\{Y\} \quad (23)$$

The soil displacement at the pile tip is:

$$\rho_b^s = \frac{S_b^s}{D_p} = \left[\left[{}_1IF_j^{sb}\right] + \left[{}_2IF_j^{sb}\right] - \kappa\left[{}_1IF_j^{sbim}\right] - \kappa\left[{}_2IF_j^{sbim}\right]\right] \times \left\{\frac{\tau}{E_s}\right\} = \frac{\sum_{j=1}^{j=n}\left(\left({}_1I\,F_j^{sb}\right)+\left({}_2I\,F_j^{sb}\right)-\kappa\left({}_1I\,F_j^{sbim}\right)-\kappa\left({}_2I\,F_j^{sbim}\right)\right)\tau_j}{E_s} \quad (24)$$

${}_1IF_j^{sb}$ and ${}_1IF_j^{sbim}$ and ${}_2IF_j^{sb}$ and ${}_2IF_j^{sbim}$ are the displacements influencing coefficients for the tip due to shear stress on real and imaginary elements 'j' of own and alongside GP, respectively. But due to uniformity ${}_1IF_j^{sb} = {}_1IF_j^{sbim}$ and ${}_2IF_j^{sb} = {}_2IF_j^{sbim}$. The new values of non-dimensional parameter, κ, is obtained as:

$$\kappa = 1 - \frac{\pi\left(1-\nu_b^2\right)p_b}{4\left(\frac{E_{sb}}{E_s}\right)\sum_{j=1}^{j=n}\tau_j\left(\left({}_1I\,F_j^{sb}\right)+\left({}_2I\,F_j^{sb}\right)\right)} \quad (25)$$

For a set of three granular piles resting on stiff bearing stratum (Eq.s (17) and (3), the interface shear stresses are

$$\left\{\frac{\tau}{E_s}\right\} = \left[\left[{}_1IF^{sp}\right] + 2\times\left[{}_2IF^{sp}\right] - \kappa\left[{}_1IF^{spim}\right] - 2\times\kappa\left[{}_2IF^{spim}\right]\right] - [\Delta]\Big]^{-1}\{Y\} \quad (26)$$

The soil displacement at the pile tip is

$$\rho_b^s = \frac{S_b^s}{D_p} = \left[\left[{}_1IF_j^{sb}\right] + 2\left[{}_2IF_j^{sb}\right] - \kappa\left[{}_1IF_j^{sbim}\right] - 2\times\kappa\left[{}_2IF_j^{sbim}\right]\right] \times \left\{\frac{\tau}{E_s}\right\} = \frac{\sum_{j=1}^{j=n}\left(\left({}_1I\,F_j^{sb}\right)+2\left({}_2I\,F_j^{sb}\right)-\kappa\left({}_1I\,F_j^{sbim}\right)-2\kappa\left({}_2I\,F_j^{sbim}\right)\right)\tau_j}{E_s} \quad (27)$$

${}_1IF_j^{sb}$ and ${}_1IF_j^{sbim}$ and ${}_2IF_j^{sb}$ and ${}_2IF_j^{sbim}$ are the displacements influencing coefficients for the tip due to shear stress on real and imaginary elements 'j' of own and alongside GP, respectively. However, due to symmetry ${}_1IF_j^{sb} = {}_1IF_j^{sbim}$ and ${}_2IF_j^{sb} = {}_2IF_j^{sbim}$. Again, the new values of non-dimensional parameter, κ, is attained as

$$\kappa = 1 - \frac{\pi\left(1-\nu_b^2\right)p_b}{4\left(\frac{E_{sb}}{E_s}\right)\sum_{j=1}^{j=n}\tau_j\left(\left({}_1I\,F_j^{sb}\right)+2\left({}_2I\,F_j^{sb}\right)\right)} \quad (28)$$

Now similarly for a set of four granular piles resting on stiff bearing stratum (Eq.s (17) and (5)) the interface shear stresses are

$$\left\{\frac{\tau}{E_s}\right\} = \begin{bmatrix}\left[{}_1IF^{sp}\right] + 2\times\left[{}_2IF^{sp}\right] + \left[{}_4IF^{sp}\right] \\ -\kappa\left[{}_1IF^{spim}\right] - 2\times\kappa\left[{}_2IF^{spim}\right] - \kappa\left[{}_4IF^{spim}\right] - [\Delta]\end{bmatrix}^{-1}\{Y\} \quad (29)$$

The soil displacement at the pile tip is:

$$\rho_b^s = \frac{S_b^s}{D_p} = \begin{bmatrix}\left[{}_1IF_j^{sb}\right] + 2\left[{}_2IF_j^{sb}\right] + \left[{}_4IF_j^{sb}\right] - \kappa\left[{}_1IF_j^{sbim}\right] - 2\times\kappa\left[{}_2IF_j^{sbim}\right] \\ -\kappa\left[{}_4IF_j^{sbim}\right]\end{bmatrix} \times \left\{\frac{\tau}{E_s}\right\} = \frac{\sum_{j=1}^{j=n}\left(\left({}_1I\,F_j^{sb}\right)+2\left({}_2I\,F_j^{sb}\right)+\left({}_4I\,F_j^{sb}\right)-\kappa\left({}_1I\,F_j^{sbim}\right)-2\kappa\left({}_2I\,F_j^{sbim}\right)-\kappa\left({}_4I\,F_j^{sbim}\right)\right)\tau_j}{E_s} \quad (30)$$

${}_1IF_j^{sb}$ and ${}_1IF_j^{sbim}$, ${}_2IF_j^{sb}$ and ${}_2IF_j^{sbim}$, and ${}_4IF_j^{sb}$ and ${}_4IF_j^{sbim}$are, respectively, the displacement influencing coefficients for the tip due to shear stresses on real and imaginary elements 'j' of own and alongside GP and fourth GP at spacing $\sqrt{2}S_p$. However due to uniformity ${}_1IF_j^{sb} = {}_1IF_j^{sbim}$ and ${}_2IF_j^{sb} = {}_2IF_j^{sbim}$. The new values of non-dimensional parameter, κ, is obtained as:

$$\kappa = 1 - \frac{\pi\left(1-\nu_b^2\right)p_b}{4\left(\frac{E_{sb}}{E_s}\right)\sum_{j=1}^{j=n}\tau_j\left(\left({}_1I\,F_j^{sb}\right)+2\left({}_2I\,F_j^{sb}\right)+\left({}_2I\,F_j^{sb}\right)\right)} \quad (31)$$

The normalized top displacement of two/three/four partly strengthened granular piles is obtained as

$$\rho_{\text{top}} = \frac{S_{\text{top}}}{D_p} = \frac{F}{\frac{\pi}{4}E_s D_p^2} D_E \quad (32)$$

The top displacement of two/three/four partly strengthened granular piles is obtained as

$$S_{\text{top}} = \frac{F}{\frac{\pi}{4}E_s D_p} D_E \quad (33)$$

Defined below are mathematical parameters which are assessed to relate the various results attained by analysis. The parameter α (displacement interaction factor) as defined by Poulos and Mattes (1971) is used (originally defined for un-strengthened set of two granular piles) and now defined as (for partly strengthened two/three/four GPs set). For set of two partly strengthened end-bearing GPs

$$\alpha_{2E} = \frac{\text{Displacement of a GP in a set of two partly strengthened GP} - \text{displacement of a single partly strengthened GP}}{\text{displacement of a single partly strengthened GP}}$$

For set of three partly strengthened end-bearing GPs

$$\alpha_{3E} = \frac{\text{Displacement of a GP in a set of three partly strengthened GP} - \text{displacement of a single partly strengthened GP}}{\text{displacement of a single partly strengthened GP}}$$

For set of four partly strengthened end-bearing GPs

$$\alpha_{4} = \frac{\text{Displacement of a GP in a set of four partly strengthened GP set} - \text{displacement of a single partly strengthened GP}}{\text{displacement by a single partly strengthened GP}}$$

Outcomes attained by carrying out ongoing analysis were termed as rigorous results.

Interaction factors for a set of three GPs are too attained from the principle of superposition as

$$\alpha_{3ES} = 2\times\alpha_{2E} \quad (34)$$

where, $\alpha_{2E,}$ is the displacement interaction factor for a set of two end-bearing GPs.

Based on the superposition principle for the interaction coefficient obtained for set of two GPs, the interaction coefficient for four GPs set is obtained as:

$$\alpha_{4ES} = 2\times\alpha_{2E}(\text{for spacing, } S_p) + \alpha_{2E}\left(\text{for spacing, } \sqrt{2}\,Sp\right) \quad (35)$$

Based on the superposition principle for the interaction coefficient obtained for set of two GPs, the interaction coefficient for four GPs set is obtained as:

$$\alpha_{4ES} = 2 \times \alpha_{2E}(\text{for spacing, } S_p) + \alpha_{2E}(\text{for spacing, } \sqrt{2}\,Sp) \quad (35)$$

where, $\alpha_{2E,}$ is displacement interaction factor for set of two ends bearing GPs.

The displacement interaction factors and D_E for the top are assessed by rigorous method and superposition principle and related with the numerous parameters previously listed as discussed in the upcoming section.

6. RESULTS AND DISCUSSION

The solutions obtained from the present analysis were found to be matching very closely with those Poulos and Mattes (1971) for an un-strengthened GP (Table 1). Simultaneously a second validation with those Madhav et al. (2019) for partial strengthened conditions is also done, as shown in Table 2. Also, the interaction factor for a set of three and four un-strengthened GPs is obtained as per superposition principle (as described above) as well as rigorous methodology and is validated with the results of Poulos and Mattes (1971) again by applying superposition principle, as depicted in Tables 3 and 4, respectively.

Table 1 Validation of values of displacement interaction factor for a set of two un-strengthened end-bearing GPs.

PARAMETERS	Set of two un-strengthened end-bearing GPs. (Interaction coefficient α)	
	Poulos & Mattes (1971)	Present study
L_p/D_p = 10, ν_{ss} = 0.5, ν_b = 0.5, S_p/D_p = 2, RSp = 10, E_{sb}/E_s = 100	0.228	0.224
L_p/D_p = 10, ν_{ss} = 0.5, ν_b = 0.5, S_p/D_p = 3, RSp = 100, E_{sb}/E_s = 100	0.068	0.066
L_p/D_p = 10, ν_{ss} = 0.5, ν_b = 0.5, S_p/D_p = 3, RSp = 1000, E_{sb}/E_s = 100	0.019	0.018

Table 2 Validation of values of displacement interaction factor for set of two partly strengthened end-bearing GPs.

PARAMETERS	Set of two partly strengthened end bearing GPs (comparison of displacement interaction factor, α)	
	Madhav et al. (2019)	Present study
E_{sb}/E_s = 100, L_p/D_p = 10, η_t = 0.3, S_p/D_p = 3, RSp = 100, χ_t = 4	0.19	0.189
E_{sb}/E_s = 100, L_p/D_p = 10, η_t = 0.3, S_p/D_p = 3, RSp = 100, χ_t = 12	0.21	0.21
E_{sb}/E_s = 10, L_p/D_p = 10, η_t = 0.3, S_p/D_p = 3, RSp = 10, χ_t = 4	0.20	0.20
E_{sb}/E_s = 10, L_p/D_p = 10, η_t = 0.3, S_p/D_p = 3, RSp = 10, χ_t = 12	0.25	0.25

Table 3 Validation of values of displacement interaction factor for set of three un-strengthened end-bearing GPs, as obtained by superposition and rigorous principle

PARAMETERS	Set of three un-strengthened end-bearing GPs. (Interaction coefficient α)		
	Poulos & Mattes (1971) as per superposition principle	Present study	
		As per superposition principle	As per rigorous principle
L_p/D_p = 10, ν_{ss} = 0.5, ν_b = 0.5, S_p/D = 2, RSp = 10, E_{sb}/E_s = 100	0.456	0.4559	0.4552
L_p/D_p = 10, ν_{ss} = 0.5, ν_b = 0.5, S_p/D_p = 3, RSp = 100, E_{sb}/E_s = 100	0.136	0.1356	0.1351

Table 4 Validation of values of displacement interaction factor for set of four un-strengthened end-bearing GPs, as obtained by superposition and rigorous principle

PARAMETERS	Set of four un-strengthened end-bearing GPs. (Interaction coefficient α)		
	Poulos & Mattes (1971) as per superposition principle	Present study	
		As per superposition principle	As per rigorous principle
L_p/D_p = 10, ν_{ss} = 0.5, ν_b = 0.5, S_p/D_p = 2, RSp = 10, E_{sb}/E_s = 100	0.778	0.777	0.772
L_p/D_p = 10, ν_{ss} = 0.5, ν_b = 0.5, S_p/D_p = 3, RSp = 100, E_{sb}/E_s = 100	0.232	0.2317	0.2311

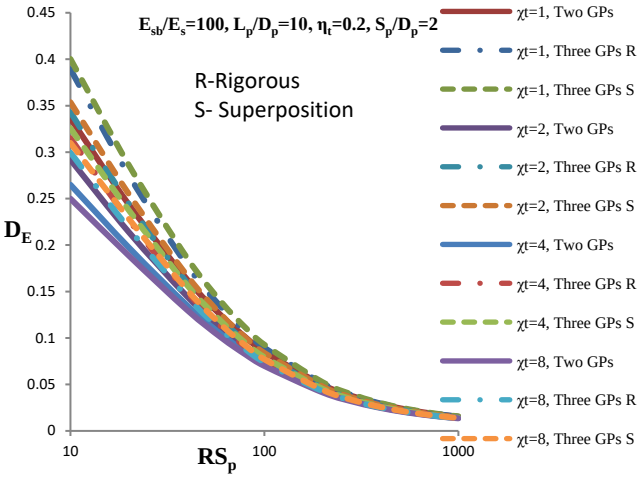

Figure 6 DEC for top of GP, D_E vs. RS_p of GP plot with influence of strengthening factor for top of GP, χ_t on a GP, in a set of two/three partly strengthened end bearing GPs (E_{sb}/E_s = 100, L_p/D_p = 10, η_t = 0.2, S_p/D_p = 2) R-rigorous, S-superposition

From Figure 6, it is observed that the DEC for top of GP, $D_{E,}$ decreases with of RS_p, GP, because as the values of RS_p of GP, increase, the engineering properties of the material of GPs, become better; hence they are able to bear the load in a better way, i.e., the load bearing capacity of the of a GP in a set of two pile set as well as three pile set increases. It can be seen from the above graph that as strengthening factor for top of GP, χ_t, increases, the DEC for top of GP, $D_{E,}$ decreases and clearly shows the favorable effect of strengthening i.e., the very purpose of strengthening is to increase the load bearing capacity which is implied here in terms of reduction in the values of top displacement. Also, the comparison between two and three pile sets reveals that the top displacement for a pile in a set of three partly strengthened set of is more than that of a pile in a set of two for any values of strengthening factor for top of GP, χ_t, It can also be observed that the values of, DEC for top of GP, $D_{E,}$ as obtained by rigorous analysis are well in synchronization with that of values obtained by superposition principle. E.g. in this case, for a set of two partly strengthened GPs with, $E_{sb}/E_s = 100$, $L_p/D_p = 10$, $\eta_t = 0.2$, $S_p/D_p = 2$, $RS_p = 100$, and $\chi_t = 1, 2, 4$, and 8, the values of, DEC for top of GP, D_E are 0.08, 0.07, 0.07, and 0.06, respectively hence leading to a percentage decrease of 12, 12, and 25 with respect to $\chi_t = 0.1$, while that for the case of set of three partly strengthened GPs with, $E_{sb}/E_s = 100$, $L_p/D_p = 10$, $\eta_t = 0.2$, $S_p/D_p = 2$, $RS_p = 100$, and $\chi_t = 1, 2, 4$, and 8, the values of, DEC for top of GP, D_E, are 0.089, 0.080, 0.076, and 0.073, respectively thereby causing a percentage decrease of 10, 14, and 18 with respect to $\chi_t = 0.1$.

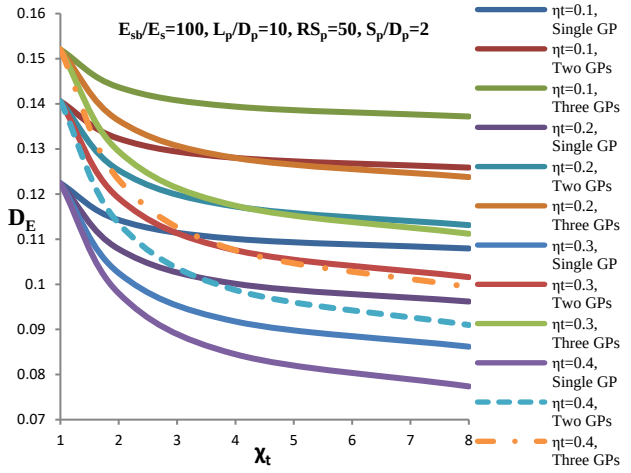

Figure 7 DEC for top of GP, D_E, vs. strengthening factor for top of GP, χ_t plot with influence of fraction of strengthened length from top of GP, η_t, on a GP, in a set of two/three partly strengthened end bearing GPs ($E_{sb}/E_s = 100$, $L_p/D_p = 10$, $RS_p = 50$, $S_p/D_p = 2$)

Figure 7 depicts that as the strengthening factor for top of GP, χ_t, is increased, the DEC for top of GP, $D_{E,}$ decreases, i.e., the basic effect and advantage of strengthening. The effect of the fraction of strengthened length from top of GP, η_t, reveals that as it increases, the values of DEC for top of GP, $D_{E,}$ decreases, which also reflects the effectiveness of strengthening while it may be deduced from the graph that as the number of piles increases the values of DEC for top of GP, $D_{E,}$ increases because by increasing the number of piles, the stress effect of one pile over the other pile in the set increases. It can be seen from the graph that, for instance, for single partly strengthened GP with, $E_{sb}/E_s = 100$, $L_p/D_p = 10$, $RS_p = 50$, $S_p/D_p = 2$, $\chi_t = 4$, and $\eta_t = 0.1, 0.2, 0.3$, and 0.4, the values of, DEC for top of GP, $D_{E,}$ are 0.11, 0.10, 0.09, and 0.08, respectively; therefore, a percentage decrease of 9, 18, and 27 occurs with respect to $\eta_t = 0.1$ while for a set of two partly strengthened GPs, with, $E_{sb}/E_s = 100$, $L_p/D_p = 10$, $RS_p = 50$, $S_p/D_p = 2$, $\chi_t = 4$, and $\eta_t = 0.1, 0.2, 0.3$, and 0.4, the values of, DEC for top of GP, $D_{E,}$ are 0.12, 0.11 0.10, and 0.09, respectively hence causing a percentage decrease of 8, 16, and 25 with respect to $\eta_t = 0.1$.

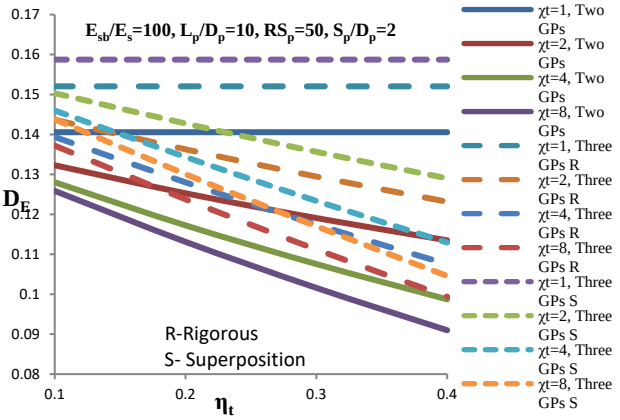

Figure 8 DEC for top of GP, D_E, vs. fraction of strengthened length from top of GP, η_t with influence of, strengthening factor for top of GP, χ_t on a GP, in a set of two/three partly strengthened end bearing GPs ($E_{sb}/E_s = 100$, $L_p/D_p = 10$, $RS_p = 50$, $S_p/D_p = 2$) R-rigorous, S-superposition

Figure 8 shows the effect of the fraction of strengthened length from top of GP, η_t and strengthening factor for top of GP, χ_t, on DEC for top of GP, D_E, and it can be seen that as a fraction of strengthened length from top of GP, η_t increases the values of DEC for top of GP, $D_{E,}$ decreases, the same trend is also observed with increase in the values of strengthening factor for top of GP, χ_t, it may also be seen that for the un-strengthened condition of the pile i.e., with $\chi_t = 1$, as expected by changing fraction of strengthened length from top of GP, η_t, there is no change in values of DEC for top of GP, D_E. While with an increase in number of piles in the set, the values of DEC for top of GP, $D_{E,}$ are found to increase as already explained. E.g., for a set of two partly strengthened GPs with, $E_{sb}/E_s = 100$, $L_p/D_p = 10$, $RS_p = 50$, $S_p/D_p = 2$, $\eta_t = 0.1$, and $\chi_t = 1, 2, 4$, and 8, the values of, DEC for top of GP, $D_{E,}$ are 0.14, 0.13, 0.12, and 0.12, respectively hence causing a percentage decrease of 7, 14, and 14 with respect to $\eta_t = 0.1$, while for a set of three partly strengthened GPs with, $E_{sb}/E_s = 100$, $L_p/D_p = 10$, $RS_p = 50$, $S_p/D_p = 2$, $\eta_t = 0.1$, and $\chi_t = 1, 2, 4$, and 8 the values of, DEC for top of GP, $D_{E,}$ are 0.15, 0.14, 0.13, and 0.13, respectively, therefore a percentage decrease of 6, 13, and 13 are observed with respect to $\eta_t = 0.1$. Here also, the two analyses carried out, viz. rigorous and superpositions, are found to be well correlated with each other.

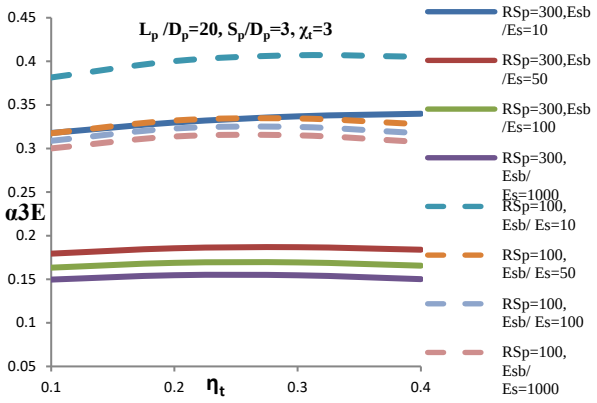

Figure 9 Displacement interaction factor, $\alpha_{3E,}$ vs. fraction of strengthened length from top of GP, η_t plot with influence of RSBS, E_{sb}/E_s, and RS_p of GP, on a GP, in a set of three partly strengthened end bearing GPs ($L_p/D_p = 20$, $S_p/D_p = 3$, $\chi_t = 3$)

Figure 9 screens the effect of RSBS, E_{sb}/E_s, and RS_p of GP, on the values of displacement interaction factor, α_{3E}. It can be seen that as RSBS, E_{sb}/E_s, increases, the values of displacement interaction factor, α_{3E}, decreases. Now since the displacement interaction factor, α_{3E} is defined as ratio of the difference between the displacement of a GP in a set of three partly strengthened GP and displacement of single partly strengthened GP to the displacement of single partly strengthened GP, so as observed from the graph the values of top displacement for both cases i.e., single GP and set of three GPs decreases with increasing RSBS, E_{sb}/E_s, but it can be simultaneously realized that the decrease is relatively more in case of three set of piles, hence the effect on displacement interaction factor, α_{3E}. Similarly, due to increase in the RS_p of the GP, the value of displacement interaction factor, α_{3E}, decreases owing to better material conditions of the GP. It has been observed, for example, that for $L_p/D_p = 20$, $S_p/D_p = 3$, $\chi_t = 3$, $\eta_t = 0.1$ with $RS_p = 300$, and $E_{sb}/E_s = 10$, 50, 100, and 1000, the values of α_{3E}, are 0.31, 0.17, 0.16, and 0.15, respectively, therefore, a percentage decrease of 45, 48, and 51 occur with respect to $E_{sb}/E_s = 10$, while for the case of, $L_p/D_p = 20$, $S_p/D_p = 3$, $\chi_t = 3$, $\eta_t = 0.1$, $RS_p = 100$, and $E_{sb}/E_s = 10$, 50, 100, and 1000, the values of, α_{3E}, are 0.38, 0.31, 0.30, and 0.30, respectively thereby causing a percentage decrease of 18, 21, and 21, with respect to $E_{sb}/E_s = 10$.

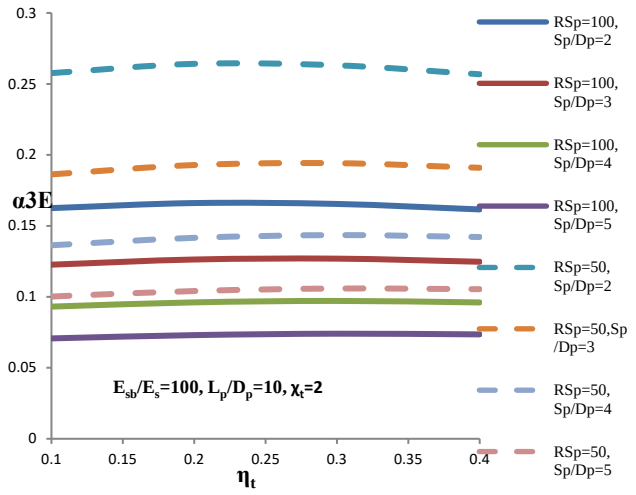

Figure 10 Displacement interaction factor, α_{3E}, vs. fraction of strengthened length from top of GP, η_t plot with influence of normalized spacing, S_p/D_p and RS_p of GP, on a GP, in a set of three partly strengthened end bearing GPs ($E_{sb}/E_s = 100$, $L_p/D_p = 10$, $\chi_t = 2$)

Figure 10 depicts the effect of normalized spacing, S_p/D_p,and RS_p of GP, on displacement interaction factor, α_{3E}. It is seen that as the values of normalized spacing, S_p/D_p, increase, the values of displacement interaction factor, α_{3E}, decrease because the influence of stresses of one pile over the other decreases as they are moving apart with increasing normalized spacing, S_p/D_p. Although the influence of RS_p of GP, is as already explained in the previous figure. For instance, it may be noted that for, $E_{sb}/E_s = 100$, $L_p/D_p = 10$, $\chi_t = 2$, $\eta_t = 0.1$ with $RS_p = 100$, and $S_p/D_p = 2$, 3, 4, and 5, the values of α_{3E}, are 0.16, 0.12, 0.09, and 0.07, respectively hence a percentage decrease of 25, 43, and 56 take place with respect to, $S_p/D_p = 2$, while for, $E_{sb}/E_s = 100$, $L_p/D_p = 10$, $\chi_t = 2$, $\eta_t = 0.1$, $RS_p = 50$, and $S_p/D_p = 2$, 3, 4, and 5, the values of, α_{3E}, are 0.25, 0.18, 0.13, and 0.10, respectively thereby causing a percentage decrease of 28, 48, and 60 with respect to, $S_p/D_p = 2$.

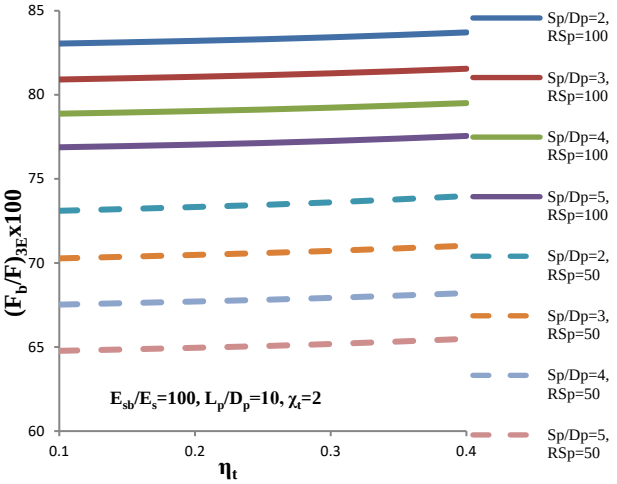

Figure 11 PLSB, $(F_b/F)_{3E}x100$, vs. fraction of strengthened length from top of GP, η_t plot with influence of normalized spacing, S_p/D_p and RS_p of GP, on a GP, in a set of three partly strengthened end bearing GPs ($E_{sb}/E_s = 100$, $L_p/D_p = 10$, $\chi_t = 2$)

Figure 11 depicts the variation of another new parameter, namely PLSB, $(F_b/F)_{3E}x100$ (PLSB of a GP in a set of three partly strengthened end bearing GPs), with normalized spacing, S_p/D_p, which, when increase leads to lowering the values of PLSB, $(F_b/F)_{3E}x100$, due to less stress interaction between adjacent piles in the set. Similarly, for RS_p of GP, it can be well observed from the graph that as this value increases, it leads to considerable increase in the value of PLSB, $(F_b/F)_{3E}x100$, because of better conditions of GP. For example, it may be observed from the graph that for, $E_{sb}/E_s = 100$, $L_p/D_p = 10$, $\chi_t = 2$, $\eta_t = 0.1$, $RS_p = 100$, and $S_p/D_p = 2$, 3, 4, and 5, the values of, $(F_b/F)_{3E}x100$ are 83.04, 80.91, 78.87, and 76.88, respectively thereby causing a decrease of 2.1, 4.1, and 6.1, with reference to $S_p/D_p = 2$, while for, $E_{sb}/E_s = 100$, $L_p/D_p = 10$, $\chi_t = 2$, $\eta_t = 0.1$, $RS_p = 50$, and $S_p/D_p = 2$, 3, 4, and 5, the values of, $(F_b/F)_{3E}x100$ are 73.10, 70.27, 67.52, and 64.77, respectively hence decrease of 2.8, 5.5, and 8.3 occur with reference to $S_p/D_p = 2$.

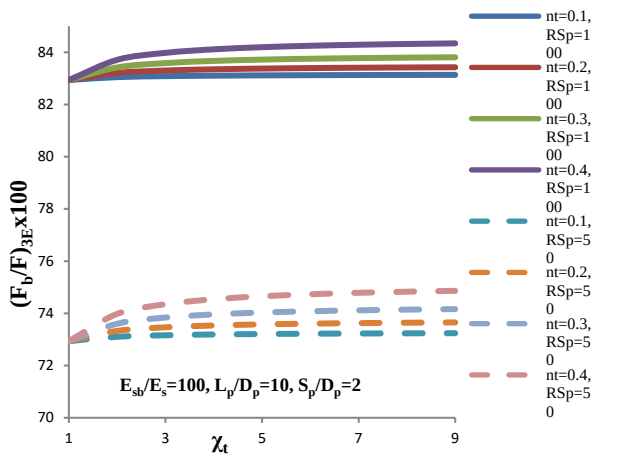

Figure 12 PLSB, $(F_b/F)_{3E}x100$, vs. strengthening factor for top of GP, χ_t plot with influence of fraction of strengthened length from top of GP, η_t, and RS_p of GP, on a GP, in a set of three partly strengthened end bearing GPs ($E_{sb}/E_s = 100$, $L_p/D_p = 10$, $S_p/D_p = 2$)

Figure 12 shows the effect of fraction of strengthened length from top of GP, η_t on PLSB, $(F_b/F)_{3E}x100$. As seen, it can be concluded that as fraction of strengthened length from top of GP, η_t, increases the PLSB,$(F_b/F)_{3E}x100$, goes on increasing owing to increment in the strengthening. Other parameter out-turn is as already described. It may well be observed from the graph that PLSB, $(F_b/F)_{3E}x100$ mainly increases in the range of strengthening factor for top of GP, χ_t = 1-3, thereafter, the graphs are more or less parallel to the horizontal axis**.** For example in this case, it may be noted that for, E_{sb}/E_s = 100, L_p/D_p = 10, S_p/D_p = 2, χ_t = 3, with RS_p = 100, and η_t = 0.1, 0.2, 0.3, and 0.4, the values of, $(F_b/F)_{3E}x100$, are, 83.08, 83.30, 83.56, and 83.97, respectively, hence causing an increase of 0.22, 0.48, and 0.89 as compared to η_t = 0.1, and for, E_{sb}/E_s = 100, L_p/D_p = 10, S_p/D_p = 2, χ_t = 3, RS_p = 50, and η_t = 0.1, 0.2, 0.3, and 0.4, the values of, $(F_b/F)_{3E}x100$, are 73.16, 73.46, 73.83, and 74.34, respectively thereby increase of, 0.3, 0.6, and 1.2 occurs as compared to η_t = 0.1.

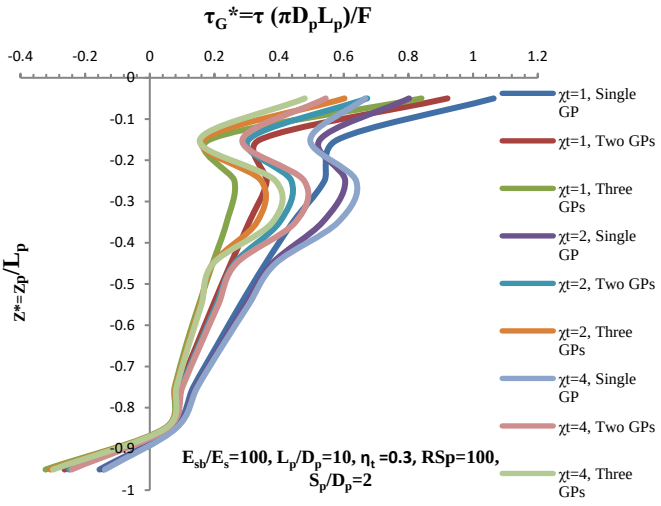

Figure 13 NSS, $\tau_G^* = \tau(\pi D_p L_p)/F$, vs. the normalized depth, $Z^* = Z_p/L_p$, plot with influence of strengthening factor for top of GP, χ_t, and comparison with single GP and set of two, three partly strengthened end bearing GPs (E_{sb}/E_s = 100, L_p/D_p = 10, η_t = 0.3, RS_p = 100, S_p/D_p = 2)

Figure 13 shows the comparative analysis of NSS, $\tau_G^* = \tau(\pi D_p L_p)/F$ on a GP in a set of two/three/four partly strengthened end bearing GPs and shows that effect is more, with more number of piles, due to pile interaction. For example, it can be seen from graph that for single partly strengthened GP, with E_{sb}/E_s = 100, L_p/D_p = 10, η_t = 0.3, RS_p = 100, S_p/D_p = 2, with, Z_p/L_p = -0.15, and χ_t = 1, 2, and 4, the values of, τ^*_{1G} = $\tau(\pi d_p L_p)/F$, (NSS of a single partly strengthened end bearing GP)are 0.58, 0.52, and 0.49, respectively hence causing a percentage decrease of 10, and 15 as compared to un-strengthened conditions, and for the case of a GP in a set of two partly strengthened GPs, for, E_{sb}/E_s = 100, L_p/D_p = 10, η_t = 0.3, RS_p = 100, S_p/D_p = 2, Z_p/L_p = -0.15, and χ_t = 1, 2, and 4, the values of, τ^*_{2G} = $\tau(\pi d_p L_p)/F$, (NSS of a GP in a set of two partly strengthened end bearing GPs) are 0.34, 0.30, and 0.28, respectively thereby causing a percentage decrease of 11 and 17 as compared to un-strengthened conditions.

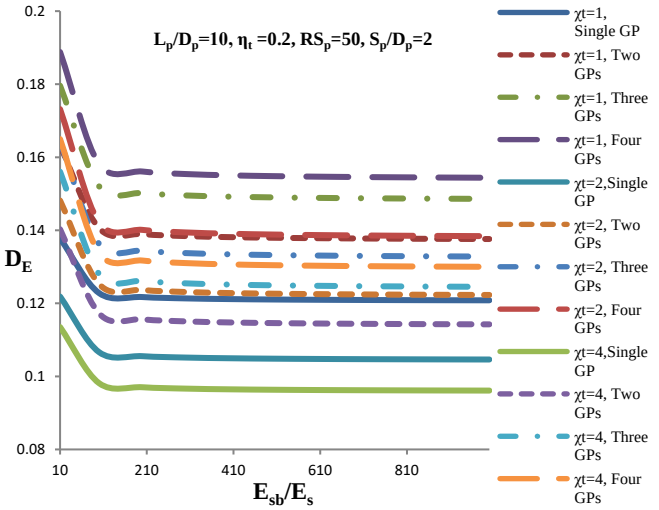

Figure 14 DEC for top of GP, D_E, vs. RSBS, E_{sb}/E_s plot with influence of strengthening factor for top of GP, χ_t, on a single GP and on a GP, in a set of two/three/four partly strengthened end bearing GPs (L_p/D_p = 10, η_t = 0.2, RS_p = 50, S_p/D_p = 2)

Figure 14 basically compares all set arrangements considered in this study. It reveals the effect of the strengthening factor for top of GP, χ_t, on DEC for top of GP, D_E, as well as the influence of RSBS, E_{sb}/E_s. It can well be seen that with increase in the values of RSBS, E_{sb}/E_s, DEC for top of GP, D_E, decreases till a range of RSBS, E_{sb}/E_s, up to 150-200 and afterward, it is not producing any considerable effects. The effect of strengthening factor for top of GP, χ_t, is as already discussed. It can be deduced from the graph that for single GP, with L_p/D_p = 10, η_t = 0.2, RS_p = 50, S_p/D_p = 2, E_{sb}/E_s = 100andχ_t, = 1, 2, and 4, the values of, D_E, are 0.12, 0.10, and 0.09, respectively thereby causing a percentage decrease of 16.6 and 25 with respect to un-strengthened conditions of GP. In case of set of two partly strengthened GPs, with L_p/D_p = 10, η_t = 0.2, RS_p = 50, S_p/D_p = 2, E_{sb}/E_s = 100andχ_t, = 1, 2, and 4, the values of D_E, are 0.14, 0.12, and 0.11, respectively hence causing a percentage decrease of 14 and 21 with respect to un-strengthened conditions of GP. In contrast, for a set of three partly strengthened GPs, with L_p/D_p = 10, η_t = 0.2, RS_p = 50, S_p/D_p = 2, E_{sb}/E_s = 100, and χ_t = 1, 2, and 4, the values of, D_E, are 0.15, 0.14, and 0.13, respectively hence causing a percentage decrease of 6 and 13 with respect to un-strengthened conditions of GP. Similarly, for a set of four partly strengthened GPs, with L_p/D_p = 10, η_t = 0.2, RS_p = 50, S_p/D_p = 2, E_{sb}/E_s = 100, and χ_t = 1, 2, and 4, the values of, D_E, are 0.16, 0.14, and 0.13, respectively hence causing a percentage decrease of 12 and 18 with respect to un-strengthened conditions of GP. As observed previously it is again observed that as number of piles increases in the set, there is an increment in the value of DEC for top of GP, D_E, due to increased stress interaction between GPs.

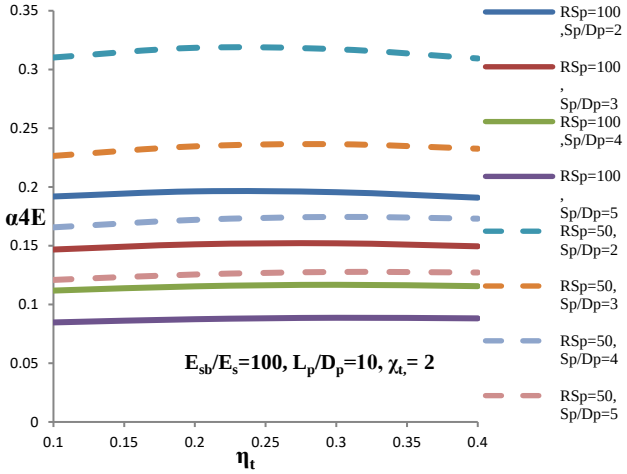

Figure 15 Displacement interaction factor, $\alpha_{4E,}$vs. fraction of strengthened length from top of GP, η_t plot with influence of normalized spacing, S_p/D_p and RS_p of GP, on a GP, in a set of four partly strengthened end bearing GPs (E_{sb}/E_s = 100, L_p/D_p = 10, χ_t = 2)

Figure 15 depicts the effect of normalized spacing, S_p/D_p, and RS_p of GP, on displacement interaction factor, α_{4E}, it may be noted that as the values of normalized spacing, S_p/D_p, increase, the values of displacement interaction factor, $\alpha_{4E,}$ decreases because the influence of stresses of one pile over the other decreases. Although the effect of RS_p of GP, is as already explained. For example, it can be seen from the graph that for, E_{sb}/E_s = 100, L_p/D_p = 10, $\chi_{t,}$ = 2, η_t = 0.4, with RS_p = 100, and S_p/D_p = 2, 3, 4, and 5, the values of, $\alpha_{4E,}$ are 0.19, 0.14, 0.11, and 0.8, respectively hence causing a percentage decrease of 26, 42, and 57 with respect to S_p/D_p = 2 while for, E_{sb}/E_s = 100, L_p/D_p = 10, $\chi_{t,}$ = 2, η_t = 0.4, RS_p = 50, and S_p/D_p = 2, 3, 4, and 5, the values of, $\alpha_{4E,}$ are 0.30, 0.23, 0.17, and 0.12, respectively thereby causing a lower percentage decrease (as compared to RS_p = 100) of 23, 43, and 60 with respect to S_p/D_p = 2.

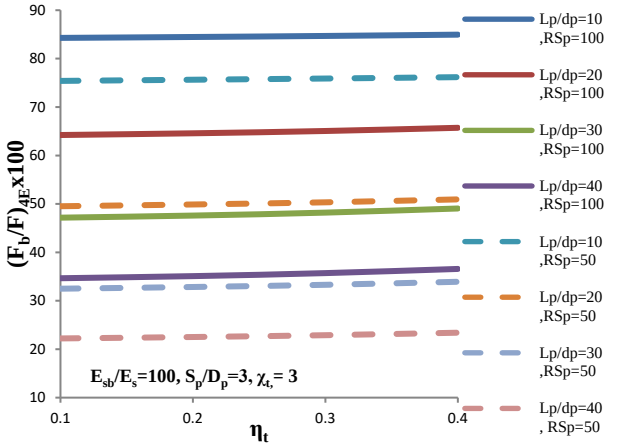

Figure 16 PLSB,$(F_b/F)_{4E}$x100, vs. fraction of strengthened length from top of GP, η_t plot with influence of relative length, L_p/D_p, and RS_p of GP, on a GP, in a set of four partly strengthened end bearing GPs (E_{sb}/E_s = 100, S_p/D_p = 3, χ_t = 3)

Figure 16 shows the effect of relative length, L_p/D_p, RS_p of GP, and fraction of strengthened length from top of GP, η_t, on PLSB,$(F_b/F)_{4E}$x100(PLSB of a GP in a set of four partly strengthened end bearing GPs) and the variations implies that the values of PLSB,$(F_b/F)_{4E}$x100, are increased by increasing fraction of strengthened length from top of GP, η_t, RS_p of GP, while a reverse trend is observable with relative length, L_p/D_p because by increasing the relative length the load transfer characteristic of the GP decreases.

As an example, it can be seen from the graph that for, E_{sb}/E_s = 100, S_p/D_p = 3, $\chi_{t,}$ = 3, η_t = 0.2, with, RS_p = 100, and L_p/D_p = 10, 20, 30, and 40, the values of, $(F_b/F)_{4E}$x100, are 84.47, 64.58, 47.59, and 35.09, respectively, therefore, decrease of 19.8, 36.8, and 49.38 occur as compared to, L_p/D_p = 10, while for, E_{sb}/E_s = 100, S_p/D_p = 3, $\chi_{t,}$ = 3, η_t = 0.2, RS_p = 50, and L_p/D_p = 10, 20, 30, and 40, the values of, $(F_b/F)_{4E}$x100, are 75.64, 49.88, 32.84, and 22.51, respectively thereby causing a decrease of 25.76, 42.8, and 53.13 as compared to, L_p/D_p = 10.

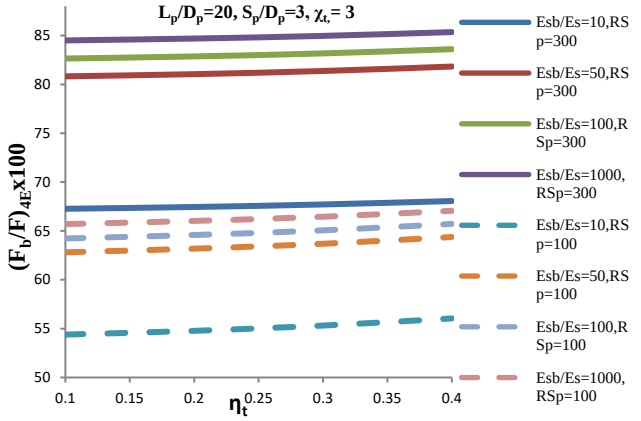

Figure 17 PLSB, $(F_b/F)_{4E}$x100, vs. fraction of strengthened length from top of GP, η_t plot with influence of RSBS, E_{sb}/E_s and RS_p of GP, on a GP, in a set of four partly strengthened end bearing GPs (L_p/D_p = 20, S_p/D_p = 3, χ_t = 3)

Figure 17 shows the trends and effect of RSBS, $E_{sb}/E_{s,}$ on PLSB, $(F_b/F)_{4E}$x100. As observable from the graph that by increasing RSBS, $E_{sb}/E_{s,}$ the PLSB, $(F_b/F)_{4E}$x100, increases. Rest trends are the same. It may well be noticed from the graph that in this case, for L_p/D_p = 20, S_p/D_p = 3, $\chi_{t,}$ = 3, η_t = 0.1, with RS_p = 100, and E_{sb}/E_s = 10, 50, 100, and 1000, the values of, $(F_b/F)_{4E}$x100, are 67.26, 80.82, 82.64, and 84.49, respectively, therefore, decrease of 13.5, 15.3, and 17.2 happens with respect to E_{sb}/E_s = 10, on the contrary for, L_p/D_p = 20, S_p/D_p = 3, $\chi_{t,}$ = 3, η_t = 0.1, RS_p = 50, and E_{sb}/E_s = 10, 50, 100, and 1000, the values of, $(F_b/F)_{4E}$x100, are 54.39, 61.81, 64.23, and 65.70, respectively thereby causing decrease of 7.4, 9.8, and 11.3 in reference to E_{sb}/E_s = 10.

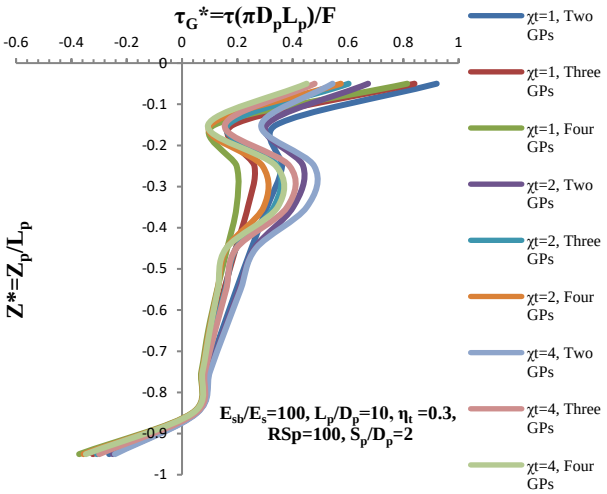

Figure 18 NSS, $\tau_G^* = \tau(\pi D_p L_p)/F$, vs. the normalized depth, $Z^* = Z_p/L_{p,}$ plot with influence of strengthening factor for top of GP, χ_t,and comparison with set of two, three and four partly strengthened end bearing GPs (E_{sb}/E_s = 100, L_p/D_p = 10, η_t = 0.3, RS_p = 100, S_p/D_p = 2)

Figure 18 shows the comparative analysis of NSS, $\tau_G^* = \tau(\pi D_p L_p)/F$, on a GP in a set of two/three/four partly strengthened end bearing GPs, and shows that effect on values of NSS, $\tau_G^* = \tau(\pi D_p L_p)/F$ is more with more number of piles. E.g., it can be observed that for set of two partly strengthened GPs with, $E_{sb}/E_s = 100$, $L_p/D_p = 10$, $\eta_t = 0.3$, $RS_p = 100$, $S_p/D_p = 2$, with, $Z_p/L_p = -0.15$, and $\chi_t = 1$, 2, and 4, the values of, $\tau_{2G}^* = \tau(\pi D_p L_p)/F$, are 0.34, 0.30, and 0.28, respectively and for set of three partly strengthened GPs with, $E_{sb}/E_s = 100$, $L_p/D_p = 10$, $\eta_t = 0.3$, $RS_p = 100$, $S_p/D_p = 2$, $Z_p/L_p = -0.15$, and $\chi_t = 1$, 2, and 4, the values of, $\tau_{3G}^* = \tau(\pi D_p L_p)/F$, (NSS of a GP in a set of three partly strengthened end bearing GPs) are 0.18, 0.16, and 0.15, respectively while for set of four partly strengthened GPs with, $E_{sb}/E_s = 100$, $L_p/D_p = 10$, $\eta_t = 0.3$, $RS_p = 100$, $S_p/D_p = 2$, with, $Z_p/L_p = -0.15$, and $\chi_t = 1$, 2, and 4, the values of, $\tau_{4G}^* = \tau(\pi D_p L_p)/F$, (NSS of a GP in a set of four partly strengthened end bearing GPs) are 0.12, 0.10, and 0.09, respectively.

7. CONCLUSIONS

A partly strengthened set of two, three and four end-bearing GPs, resting on a bearing stratum, is analyzed using the basic mirror image method and basic integration scheme of Mindlin's equation.

1. In the event of a set of two partly strengthened end-bearing GPs, it was observed that as the strengthening factor for top of GP, χ_t, increases from 1 to 8, for the $RS_p = 100$, relative length, $L_p/D_p = 10$, RSBS, $E_{sb}/E_s = 100$, normalized spacing, $S_p/D_p = 2$ and fraction of strengthened length from top of GP, $\eta_t = 0.2$ there is a reduction in displacement effecting component for top of GP, D_E, by 25%, while for set of three partly strengthened end bearing GPs for the same conditions the reduction in value of D_E is of the order of 18%. Hence reduction in displacement effecting component for top of GP is more for set of two partly strengthened end-bearing GPs as compared to later.
2. With the increase in fraction of strengthened length from top of GP, η_t from 0.1 to 0.4, for relative length, $L_p/D_p = 10$, RSBS, $E_{sb}/E_s = 100$, normalized spacing, $S_p/D_p = 2$, $RS_p = 50$, strengthening factor for top of GP, $\chi_t = 2$ displacement effecting component for top of GP, D_E, for a group of two partly strengthened end bearing GPs decreases by14%, while for the set of three partly strengthened end bearing GPs, for the same conditions the reduction in value of D_E is 13%. Therefore, as the η_t increases, the value of D_E tends to decrease but the reduction in displacement effecting component for top of GP is seen more in a set of two partly strengthened end-bearing GPs than the latter.
3. The displacement interaction factor, α_{3E}, is observed to decrease with an increase in RS_p and E_{sb}/E_s. For instance, at $L_p/D_p = 20$, $S_p/D_p = 3$, $\chi_t = 3$, $\eta_t = 0.1$ with $RS_p = 300$, and $E_{sb}/E_s = 10$, and 1000, the value of α_{3E}, is 0.31and 0.15, respectively; hence a percentage decrease of 51 happens with respect to $E_{sb}/E_s = 10$, while for the case of, $L_p/D_p = 20$, $S_p/D_p = 3$, $\chi_t = 3$, $\eta_t = 0.1$ with, $RS_p = 100$, and $E_{sb}/E_s = 10$, and 1000 the values of, α_{3E}, is 0.38 and 0.30, respectively thereby producing a percentage decrease of 21 with respect to $E_{sb}/E_s = 10$. Therefore, as the value of RS_p increases, the α_{3E}tend to decrease.
4. It is observed that with an increase in normalized spacing, S_p/D_p, the displacement interaction factor, α_{3E}, decreases because the pile will be at a long distance, so the effect of stresses will also decrease. Similarly, α_{4E}, also tends to decrease with an increase in S_p/D_p. But in case of a set of four partly strengthened end-bearing GPs decrease is more than that set of three partly strengthened end GPs. For instance, for $E_{sb}/E_s = 100$, $L_p/D_p = 10$, $\chi_t = 2$, $\eta_t = 0.1$ with, RSp = 100, and $S_p/D_p = 5$ the values of, α_{3E}, is 0.07 while for α_{4E}, it is 0.8.
5. For the set of three partly strengthened end-bearing GPs, the value of PLSB, $(F_b/F)_{3E}$x100 decreases, with an increase in normalized spacing, S_p/D_p, because of less stress impact between adjacent piles in the set, but with the increase in the fraction of strengthened length from top of GP, η_t the value of PLSB, $(F_b/F)_{3E}$x100 tend to increase, ultimately leading to beneficial effect of strengthening.
6. For the set of four partly strengthened end-bearing GPs, the value of PLSB, $(F_b/F)_{4E}$x100 decreases at the value of $RS_p = 100$, with an increase in relative length, L_p/D_p, because the load transfer mechanism of GP decrease, but with the increased in the RSBS, E_{sb}/E_s, the value of PLSB, $(F_b/F)_{4E}$x100 tend to increase.
7. In the event of a single and set of two, three, or four partly strengthened end-bearing GPs, it was found that as the strengthening factor for top of GP, χ_t, increases from 1 to 4 for the $RS_p = 100$, relative length, $L_p/D_p = 10$, RSBS, $E_{sb}/E_s = 100$, normalized spacing, $S_p/D_p = 2$, a fraction of strengthened length from top of GP, $\eta_t = 0.3$ at a depth of 0.15 the value of NSS, $\tau_G^* = \tau(\pi D_p L_p)/F$ on a GP in a set of two/three/four partly strengthened end bearing GPs, decreases. The decrease in value of NSS for the set of four partly strengthened end bearing GP is more than the other three, viz. one, two, and three partly strengthened end-bearing GPs.

8. ACKNOWLEDGMENT

The authors are highly grateful to the late Dr. Vaibhaw Garg, Associate Professor, Civil Engineering Department, Rajasthan Technical University, Kota and would like to acknowledge the suggestions and discussions held with him. Unfortunately, he lost his life due to Covid-19.

9. REFERENCES

Amgir, M., Miura, N., Poorooshasb, H. B., & Madhav, M. R. (1996). "Deformation analysis of soft ground reinforced by columnar inclusions". Computers and geotechnics, 18(4), 267-290.

Garg, V., & Sharma, J. K. (2019). "Analysis and settlement of partially stiffened single and group of two floating granular piles". Indian Geotechnical Journal, 49(2), 191-203.

Madhav, M. R., & Nagpure, D. D. (1995). "Granular piles- A low-cost alternative to R. C. C. Piles". In Proc. of National seminar on Ground Improvement Techniques. GRIMTECH, Indore, pp. 17-29.

Madhav, M. R., Sharma, J. K., & Chandra, S. (2006). "Analysis and settlement of a non-homogeneous granular pile". Indian Geotechnical Journal, 36(3), 249-271.

Madhav, M.R., Sharma, J.K., Garg, V (2019). "Stiffening effect on end bearing granular piles" A special issue Honouring Dr. Bengt. Fellenius". Geotechnical Engineering Journal of the SEAGS and AGSSEA 50(3), pp. 32-40.

Mattes, N. S., & Poulos, H. G. (1969). "Settlement of single compressible pile". Journal of the Soil Mechanics and Foundations Division, 95(1), 189-207.

Mindlin, R. D. (1936). "Force at a point in the interior of a semi-infinite solid". Physics, *7*(5), 195-202.

Mindlin, R. D. (1937). "Stress system in a circular disk under radial forces", presented at the joint meeting of applied mechanics and hydraulic division of the ASME held at Cornell University, NY, pp. A115–118.

Murugesan, S., & Rajagopal, K. (2006). "Geosynthetic-encased stone columns: numerical evaluation". Geotextiles,and Geomembranes, 24(6), 349-358.

Najjar, S. S., & Skeini, H. (20). "Triaxial response of clays reinforced with granular columns 15". Proceedings of the Institution of Civil Engineers-Ground Improvement, 168(4), 265-281.

Poorooshasb, H. B., Miura, N., and Noorzad, A. (1998). "An upper bound analysis of the behavior of stone columns". Lecture presented at Saga University, Saga, Japan, pp. 7-37.

Poulos, H. G., & Mattes, N. S. (1971). "Settlement and load distribution analysis of pile groups". Australian Geomechanics Journal, 1(1).

Pulko, B., & Majes, B. (2005). "Simple and accurate prediction of settlements of stone column reinforced soil" in proceedings of the International conference on soil mechanics and geotechnical engineering (vol. 16, no. 3, p. 1401). AA Balkema Publishers.

Shahu, J. T., & Reddy, Y. R. (2011). "Clayey soil reinforced with stone column group: model tests and analyses". Journal of Geotechnical and Geoenvironmental Engineering, 137(12), 1265-1274.

Sivakumar, V., McKelvey, D., Graham, J., & Hughes, D. (2004). "Triaxial tests on model sand columns in clay". Canadian Geotechnical Journal, 41(2), 299-312.

Zhang, Y., Chan, D., & Wang, Y. (2012). "Consolidation of composite foundation improved by geosynthetic-encased stone columns". Geotextiles and Geomembranes, 32, 10-17.